

# Size effects on charge ordering and magnetic properties in $\text{La}_{0.25}\text{Ca}_{0.75}\text{MnO}_3$

X.G. Li <sup>a,b,\*</sup>, T. Zhang <sup>a,b</sup>

<sup>a</sup> Hefei National Laboratory for Physical Sciences at Microscale, Department of Physics, University of Science and Technology of China, Anhui, Hefei 230026, China

<sup>b</sup> International Center for Materials Physics, Academia Sinica, Shenyang 110015, China

Accepted 1 October 2007

Available online 23 December 2007

## Abstract

The size effects on the charge ordering (CO) and magnetic properties in  $\text{La}_{0.25}\text{Ca}_{0.75}\text{MnO}_3$  with mean particle size ranging from 40 to 2000 nm were studied. With decreasing particle size the CO transition temperature shifts to lower temperature and the transition width becomes increasingly wide, indicating the weakening of the CO state. Meanwhile the ferromagnetic (FM) cluster glass state appears and the magnetization at low temperature increases significantly. The behaviour is due to the increasing uncompensated surface spins which weaken the antiferromagnetic interaction and disfavour the formation of the CO state. The suppression of the CO state and appearance of the FM cluster glass state are also found in  $\text{La}_{0.25}\text{Ca}_{0.75}\text{MnO}_3$  nanowires fabricated by a sol–gel template method. These results indicate that the CO state can be modulated effectively by varying particle size, which has an important implication for nano-device applications of manganites.

© 2007 Elsevier Ltd and Techna Group S.r.l. All rights reserved.

**Keywords:** C. Magnetic properties; Charge ordering; Manganites

## 1. Introduction

Doped manganites have attracted much attention because of their rich physics and potential applications [1–3]. The charge ordering (CO) phenomenon, accompanied with the localization of  $e_g$  electrons and appearance of the antiferromagnetic (AFM) spin ordering below the CO transition temperature  $T_{\text{CO}}$ , represents one of the most interesting issues in these materials due to the strong interactions among the charge, orbital, spin and lattice degrees of freedom [4–6]. The CO state can be controlled by chemical and physical methods. For example, the substitution of non-magnetic impurities Al for Mn in  $\text{Pr}_{0.5}\text{Ca}_{0.5}\text{MnO}_3$  suppresses the CO and reduces the AFM transition temperature [7]; a high external pressure destroys the low-temperature CO insulating state and induces a ferromagnetic (FM) metallic state in  $\text{Pr}_{1-x}\text{Ca}_x\text{MnO}_3$  system due to the increase of the bandwidth [8]. In our previous studies, it was

found that for the phase separated  $\text{La}_{0.5}\text{Ca}_{0.5}\text{MnO}_3$  magnetic fields make  $T_{\text{CO}}$  shift to lower temperature and a field of 12 T can melt the CO state completely, while for  $\text{La}_{0.25}\text{Ca}_{0.75}\text{MnO}_3$ , the CO state is very stable and insensitive to magnetic field even up to 14 T [9]. For charge ordered AFM materials, when their size is reduced to nanoscale, the uncompensated surface spins will destroy the perfect AFM configuration and weaken the AFM interaction [10], which would impede the formation of the CO state [11]. This may provide a distinct method to modulate the CO state and magnetic properties of manganites by varying particle size.

In the present work, the effects of particle size on the CO and magnetic properties of  $\text{La}_{0.25}\text{Ca}_{0.75}\text{MnO}_3$  were studied. With decreasing particle size, the suppression of the CO state and appearance of the FM cluster glass state were observed. In addition, such an anomalous behaviour was also found in  $\text{La}_{0.25}\text{Ca}_{0.75}\text{MnO}_3$  nanowires with an average diameter of 60 nm prepared using a sol–gel template method.

## 2. Experimental procedure

Polycrystalline  $\text{La}_{0.25}\text{Ca}_{0.75}\text{MnO}_3$  samples were prepared by a sol–gel method. The stoichiometric amounts of  $\text{La}_2\text{O}_3$

\* Corresponding author at: Hefei National Laboratory for Physical Sciences at Microscale, Department of Physics, University of Science and Technology of China, Anhui, Hefei 230026, China. Tel.: +86 551 3602196; fax: +86 551 3603408.

E-mail address: [lixg@ustc.edu.cn](mailto:lixg@ustc.edu.cn) (X.G. Li).

(99.9%),  $\text{CaCO}_3$  (99.5%) and 50%  $\text{Mn}(\text{NO}_3)_2$  solution were used as starting materials.  $\text{La}_2\text{O}_3$  and  $\text{CaCO}_3$  were converted into metal nitrates by adding nitric acid. These metal nitrates and excessive EDTA were dissolved in distilled water to obtain a clear solution with an initial molar ratio of  $\text{La}:\text{Ca}:\text{Mn} = 1:3:4$ . The pH of solution was adjusted to 6–7 by adding ethylenediamine, and then appropriate amount of ethylene glycol was added to the solution. Subsequently the solution was heated with stirring to evaporate most of the solvent water. The resultant sol-precursors were decomposed firstly at about  $300^\circ\text{C}$  and the obtained precursor powder was separated into several parts and annealed at different temperatures from 600 to  $1280^\circ\text{C}$  to get samples with different particle sizes. The synthesis process of nanowires is similar to that reported in our previous work [12]. The structure characterization was performed by X-ray diffractometer (XRD) (MXP18AHF). The average particle size and morphology were characterized by a field emission scanning electron microscopy (FE-SEM) (JSM-6700F). The magnetic properties were measured by a superconducting quantum interference device (SQUID) (MPMS) magnetometer.

### 3. Results and discussion

The average particle diameter  $D$  determined by FE-SEM as a function of the thermal treatment temperature ( $T_a$ ) is plotted in Fig. 1, in which  $D$  increases from 40 to 2000 nm with increasing  $T_a$  from 600 to  $1280^\circ\text{C}$ . Fig. 2 shows the temperature dependence of the zero field cooled (ZFC) magnetization measured on warming under a magnetic field of 5 T for  $\text{La}_{0.25}\text{Ca}_{0.75}\text{MnO}_3$  compounds with different particle sizes. With decreasing temperature, the magnetizations increase firstly and then decrease rapidly after reaching a maximum, signalling the development of the CO state for all samples, which is similar to that observed for the bulk  $\text{La}_{0.25}\text{Ca}_{0.75}\text{MnO}_3$  sample [13,14]. The peak in the magnetization curve is related to the change from the weakly ferromagnetically correlated Mn spins to the antiferromagnetically correlated ones due to the developments of the charge and orbital orderings [13]. For the 2000 nm sample,  $T_{\text{CO}}$  of about 240 K, defined as the peak

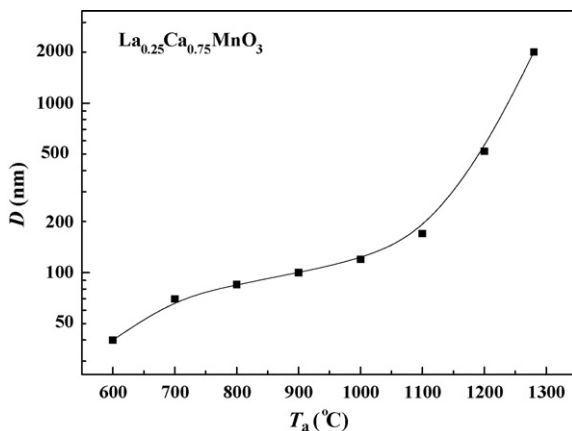


Fig. 1. Average particle size ( $D$ ) determined by FE-SEM as a function of thermal treatment temperature ( $T_a$ ). The line is a guide to eyes.

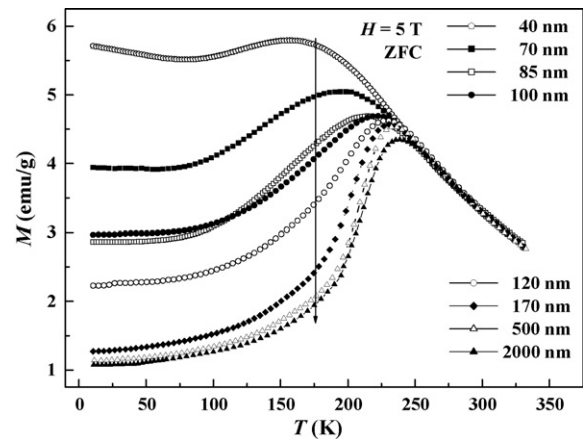


Fig. 2. Temperature dependencies of the magnetizations of  $\text{La}_{0.25}\text{Ca}_{0.75}\text{MnO}_3$  samples with different average particle sizes measured under 5 T in ZFC mode. The arrow shows the direction for the increase of the particle size.

temperature of the  $M$  vs.  $T$  curves, is consistent with that of the bulk material [15], and the transition is very steep. With decreasing particle size, the  $T_{\text{CO}}$  obtained under 5 T shifts gradually to lower temperature, and the transition width becomes increasingly wide, which clearly indicates the weakening of the CO state. Meanwhile the magnetization at low temperature increases significantly. This behaviour can be explained according to a core–surface model proposed by Bhowmik et al. [10]. For AFM nanoparticles, the core spins are almost antiparallel with the exchange energy  $E_{\text{ex}} = -1$ , while the deviation of the surface spins from the AFM arrangement leads to the uncompensated surface spins and thereby results in higher net moments [16] and makes the  $E_{\text{ex}}$  value be less negative at the surface regions. With decreasing particle size, the influence of the uncompensated surface spins increases due to the increase of surface/volume ratio. As a result, the magnetization at low temperature increases and the AFM interaction weakens gradually, which disfavours the formation of the CO state [11,17] and induces the decrease of the  $T_{\text{CO}}$ . Moreover, the uncompensated surface spins give rise to an inhomogeneous spatial distribution of the AFM interaction strength across the whole particle and hence lead to the broad CO transition increasingly.

Note that in manganites there exists strong competition between the double exchange FM interaction and the super-exchange AFM interaction. As mentioned above, the decrease of the particle size weakens the AFM interaction, which makes the free energies of FM and AFM close and may result in the formation of FM clusters in some regions [18]. In order to investigate the FM behaviour, the ZFC and field cooled (FC) magnetizations under 0.01 T were measured, as shown in Fig. 3, since the FM spins are very sensitive to a low magnetic field. For the 2000 nm sample, a sharp peak  $P_1$  around 240 K in the  $M$ – $T$  curves corresponding to the CO transition is consistent with that under 5 T. For the 500 nm sample, in addition to  $P_1$  around 236 K, an evident ascent of the FC curve below 174 K implies the enhancement of the FM fluctuations. As the particle size is reduced to 170 nm, besides  $P_1$  shifting to a lower temperature and becoming indistinct, there is another peak  $P_2$  appears around

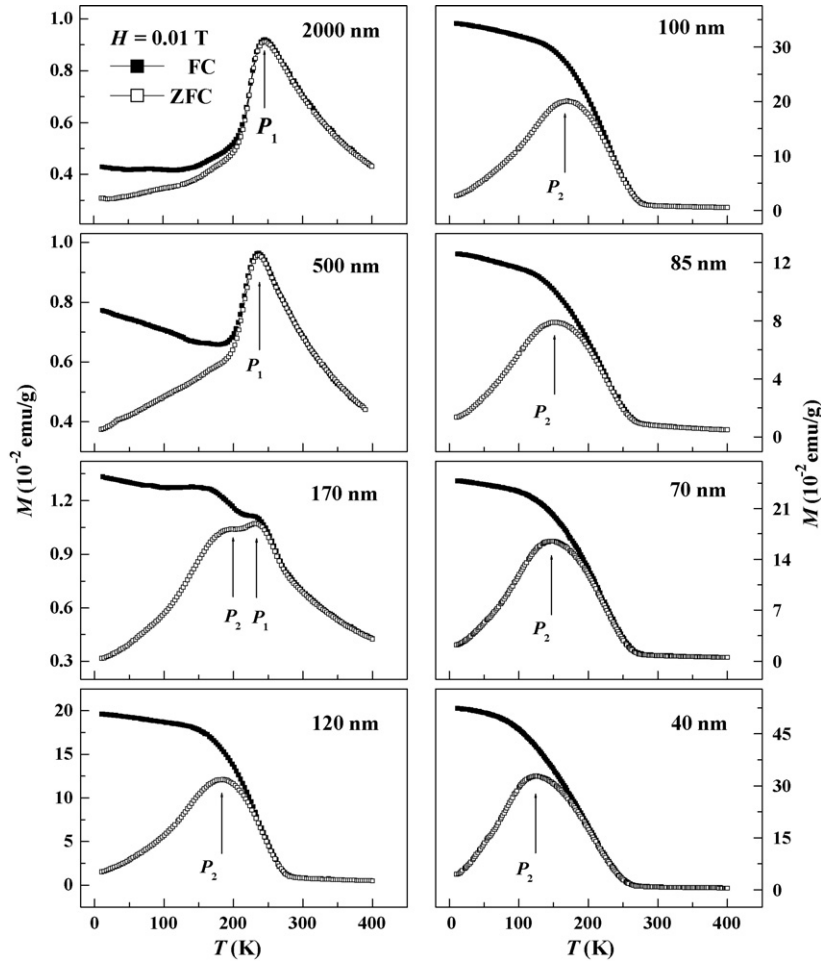


Fig. 3. Temperature dependencies of the magnetizations of  $\text{La}_{0.25}\text{Ca}_{0.75}\text{MnO}_3$  samples measured under 0.01 T in ZFC and FC modes.

196 K in the ZFC curve and the FC magnetization exhibits a rapid increase around 200 K. For the samples with particle size below 120 nm,  $P_1$  disappears and  $P_2$  becomes more obvious. The rapid increase in magnetization around a certain temperature in  $M$  vs.  $T$  curves may be related to the formation of a long-range FM order or short-range FM cluster glass. However, the ac susceptibility data in Ref. [19] indicates that it results from the latter, and the  $P_2$  position marks the freezing of the FM clusters glass [20]. As for the disappearance of  $P_1$ , it can be ascribed to the discrepancy of the sensitivity of different magnetic phases to applied magnetic fields. The reason is that, as well known, the FM cluster moments are easily polarized under 0.01 T field, while the AFM and PM susceptibilities are much lower, which leads to the cover-up of the characteristic of the CO transition due to the existence of the FM cluster glass for the particle size below 120 nm.

Based on the magnetization measurements under  $H = 0.01$  and 5 T, the particle size dependent phase diagrams for the temperature  $T_C$  (determined by the minimum of  $dM/dT$  vs.  $T$  curves under 0.01 T) of the appearance of FM clusters and  $T_{CO}$  are constructed, as shown in Fig. 4. Since the values of  $T_{CO}$  obtained under 5 T decrease rapidly for the small particle size, it can be predicted that when the particle size is reduced below a critical value ( $D_0$ ), the uncompensated surface spins will cause a fundamental change in the magnetic configuration throughout a particle, which will lead to a complete disappearance of the

CO state.  $D_0$  can be obtained by an empirical equation:

$$T_{CO}(D) = T_{CO}^b \left(1 - \frac{D_0}{D}\right)^\gamma \quad (1)$$

where  $T_{CO}^b$  is the CO transition temperature for the bulk material,  $D_0$  is the critical particle size for the disappearance

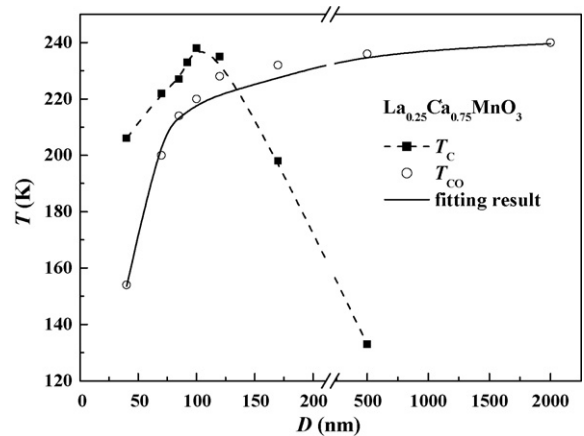


Fig. 4. The temperature vs. particle size phase diagram of  $\text{La}_{0.25}\text{Ca}_{0.75}\text{MnO}_3$ .  $T_{CO}$  and  $T_C$  obtained under 5 and 0.01 T, respectively. The dash line is a guide to eyes and the solid line is the fitted result using Eq. (1).

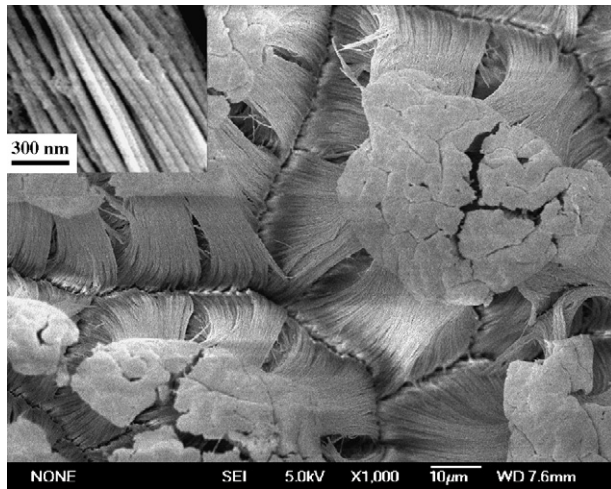


Fig. 5. The top view SEM micrograph of  $\text{La}_{0.25}\text{Ca}_{0.75}\text{MnO}_3$  nanowire arrays after removing part alumina membrane. The inset is an enlargement of a randomly selected region.

of the CO state, and  $\gamma$  is a fitting parameter. The solid line in Fig. 4 is the fitted result with  $T_{\text{CO}}^b = 241$  K,  $D_0 = 17$  nm and  $\gamma = 0.54$ . While for the variation of  $T_{\text{C}}$ , with decreasing particle size it shows a non-monotonous behaviour with a maximum at about 100 nm. This is due to the fact that the FM interaction is also disfavoured by the surface spins [21].

To further approve the size dependencies of the CO state and magnetic properties of the system, the magnetization of polycrystalline  $\text{La}_{0.25}\text{Ca}_{0.75}\text{MnO}_3$  nanowires prepared by a sol-gel template method was also measured. Fig. 5 shows a typical SEM micrograph of the as-prepared sample after removing the part alumina membrane. An enlargement of a randomly selected region of Fig. 5, as shown in the inset, indicates that the

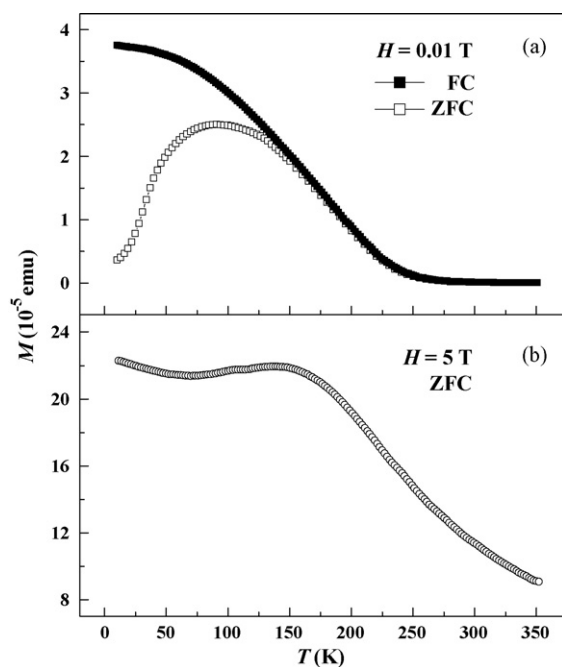


Fig. 6. Temperature dependencies of the magnetizations of  $\text{La}_{0.25}\text{Ca}_{0.75}\text{MnO}_3$  nanowires measured on warming (a) under 0.01 T after ZFC and FC processes, (b) under 5 T after ZFC process.

nanowires with a uniform diameter about 60 nm are plump. In Fig. 6, the  $M$ – $T$  curves measured under 0.01 and 5 T reveal that the CO state is suppressed and the FM cluster glass state appears in these nanowires, which support the above results in the nanoparticles.

#### 4. Conclusions

In summary, the size effects on the CO state and magnetic properties of  $\text{La}_{0.25}\text{Ca}_{0.75}\text{MnO}_3$  indicate that with decreasing particle size the increasing uncompensated surface spins weaken the AFM interaction, which suppresses the CO state and induces the appearance of the FM cluster glass state. This work provides a simple and effective method for controlling the CO state in manganites.

#### Acknowledgements

This work was supported by the National Natural Science Foundation of China (50421201 and 10334090) and the National Basic Research Program of China (2006CB922005).

#### References

- [1] Y. Tokura, Colossal Magnetoresistive Oxides, Gordon & Breach, Tokyo, 1999, pp. 1–49.
- [2] C.N.R. Rao, R. Raveau, Colossal Magnetoresistance, Charge Ordering and Related Properties of Manganese Oxides, World Scientific, Singapore, 1998.
- [3] M.B. Salamon, M. Jaime, The physics of manganites: structure and transport, Rev. Mod. Phys. 73 (3) (2001) 583–628.
- [4] C. Martin, A. Maignan, M. Hervieu, B. Raveau, Magnetic phase diagrams of  $\text{La}_{1-x}\text{A}_x\text{MnO}_3$  manganites ( $\text{L} = \text{Pr, Sm}$ ;  $\text{A} = \text{Ca, Sr}$ ), Phys. Rev. B 60 (17) (1999) 12191–12199.
- [5] H. Fujishiro, T. Fukase, M. Ikebe, Charge ordering and sound velocity anomaly in  $\text{La}_{1-x}\text{Sr}_x\text{MnO}_3$  ( $x \geq 0.5$ ), J. Phys. Soc. Jpn. 67 (5) (1998) 2582–2585.
- [6] A. Moreo, S. Yunoki, E. Dagotto, Solid state physics-phase separation for manganese oxides and related materials, Science 283 (5410) (1999) 2034–2040.
- [7] S. Nair, A. Banerjee, The effect of Al substitution on charge ordered  $\text{Pr}_{0.5}\text{Ca}_{0.5}\text{MnO}_3$ : structure, magnetism and transport, J. Phys.: Condens. Matter 16 (16) (2004) 8335–8344.
- [8] C.W. Cui, T.A. Tyson, Pressure effects on charge, spin, and metal-insulator transitions in the narrow bandwidth manganite  $\text{Pr}_{1-x}\text{Ca}_x\text{MnO}_3$ , Phys. Rev. B 70 (9) (2004) 094409–094416.
- [9] X.G. Li, R.K. Zheng, G. Li, H.D. Zhou, R.X. Huang, J.Q. Xie, Z.D. Wang, Jahn–Teller effect and stability of the charge-ordered state in  $\text{La}_{1-x}\text{Ca}_x\text{MnO}_3$  ( $0.5 \leq x \leq 0.9$ ) manganites, Europhys. Lett. 60 (5) (2002) 670–676.
- [10] R.N. Bhowmik, R. Nagarajan, R. Ranganathan, Magnetic enhancement in antiferromagnetic nanoparticle of  $\text{CoRh}_2\text{O}_4$ , Phys. Rev. B 69 (5) (2004) 054430–054434.
- [11] R.Y. Gu, Z.D. Wang, C.S. Ting, Theory of electric-field-induced metal–insulator transition in doped manganites, Phys. Rev. B 67 (15) (2003) 153103–153106.
- [12] T. Zhang, C.G. Jin, J. Zhang, X.L. Lu, X.G. Li, Microstructure and magnetic properties of  $\text{La}_{0.62}\text{Pb}_{0.38}\text{MnO}_3$  nanowire arrays, Nanotechnology 16 (11) (2005) 2743–2747.
- [13] M. Pissas, I. Margiolaki, K. Prassides, E. Suard, Crystal and magnetic structural study of the  $\text{La}_{1-x}\text{Ca}_x\text{MnO}_3$  compound ( $x = 3/4$ ), Phys. Rev. B 72 (6) (2005) 064425–064426.
- [14] R.K. Zheng, A.N. Tang, Y. Yang, W. Wang, G. Li, X.G. Li, Transport, magnetic, specific heat, internal friction, and shear modulus in the charge

- ordered  $\text{La}_{0.25}\text{Ca}_{0.75}\text{MnO}_3$  manganite, *J. Appl. Phys.* 94 (1) (2003) 514–518.
- [15] T. Qian, R.K. Zheng, T. Zhang, T.F. Zhou, W.B. Wu, X.G. Li, Effect of Jahn–Teller interactions on the specific heat and magnetic properties of charge-ordered  $\text{La}_{1-x}\text{Ca}_x\text{MnO}_3$  ( $0.55 \leq x \leq 0.87$ ), *Phys. Rev. B* 72 (2) (2005) 024432–024438.
- [16] R.H. Kodama, A. Salah, A.E. Makhlof, Berkowitz, Finite size effects in antiferromagnetic NiO nanoparticles, *Phys. Rev. Lett.* 79 (7) (1997) 1393–1396.
- [17] T. Hotta, A.L. Malvezzi, E. Dagotto, Charge-orbital ordering and phase separation in the two-orbital model for manganites: roles of Jahn–Teller phononic and Coulombic interactions, *Phys. Rev. B* 62 (14) (2000) 9432–9452.
- [18] D. Niebieskikwiat, R.D. Sánchez, A. Caneiro, B. Alascio, Phase separation in polycrystalline  $\text{Pr}_{0.5}\text{Sr}_{0.5-x}\text{Ca}_x\text{MnO}_3$ , *Phys. Rev. B* 63 (21) (2001) 212402–212405.
- [19] T. Zhang, T.F. Zhou, T. Qian, X.G. Li, Particle size effects on interplay between charge ordering and magnetic properties in nanosized  $\text{La}_{0.25}\text{Ca}_{0.75}\text{MnO}_3$ , *Phys. Rev. B* 76 (17) (2007) 174414–174421.
- [20] X.G. Li, X.J. Fan, G. Ji, W.B. Wu, K.H. Wong, C.L. Choy, H.C. Ku, Field-induced crossover from cluster-glass to ferromagnetic state in  $\text{La}_{0.7}\text{Sr}_{0.3}\text{Mn}_{0.7}\text{Co}_{0.3}\text{O}_3$ , *J. Appl. Phys.* 85 (3) (1999) 1663–1666.
- [21] M.A. López-Quintela, L.E. Hueso, J. Rivas, F. Rivadulla, Intergranular magnetoresistance in nanomanganites, *Nanotechnology* 14 (3) (2003) 212–219.